HHS Public Access

Author manuscript

J Leukoc Biol. Author manuscript; available in PMC 2023 August 01.

Published in final edited form as:

J Leukoc Biol. 2022 August ; 112(2): 221–232. doi:10.1002/JLB.4HI0921-492R.

T Cell activation and IFNγ modulate organ dysfunction in lipopolysaccharide-mediated inflammation

Matthew D. Taylor[*], **Tiago D. Fernandes**[*], **Omar Yaipen**[*], **Cassidy E. Higgins**[*], **Christine A. Capone**[*], **Daniel E. Leisman**[†], **Ana Nedeljkovic-Kurepa**[*], **Mabel N. Abraham**[*], **Mariana R. Brewer**[*], **Clifford S. Deutschman**[*]

[*]The Division of Critical Care Medicine, Department of Pediatrics, The Feinstein Institutes for Medical Research, Manhasset, NY, Cohen Children's Medical Center/Northwell Health, New Hyde Park, NY

[†]Department of Anesthesia, Critical Care, and Pain Medicine, Massachusetts General Hospital, Boston, MA

Abstract

Lipopolysaccharide (LPS) challenge is used to model inflammation-induced organ dysfunction. The effects of T cell activation on LPS-mediated organ dysfunction and immune responses are unknown. We studied these interactions through *in vivo* administration of anti-CD3ε (CD3) T cell activating antibody and LPS. Mortality in response to high-dose LPS (LPSHi; 600μg) was 60%; similar mortality was observed with a 10-fold reduction in LPS dose (LPSLo; 60μg) when administered with CD3 (CD3LPSLo). LPSHi and CD3LPSLo cohorts suffered severe organ dysfunction. CD3LPSLo led to increased IFNγ and IL12p70 produced by T cells and dendritic cells (cDCs) respectively. CD3LPSLo caused cDC expression of CD40 and MHCII and prevented PD1 expression in response to CD3. These interactions led to generation of CD4 and CD8 cytolytic T cells. CD3LPSLo responded to IFNγ or IL12p40 blockade, in contrast to LPSHi. The combination of T cell receptor activation and LPS (CD3LPSLo) dysregulated T cell activation, and increased LPS-associated organ dysfunction and mortality through T cell and cDC interactions.

Summary Sentence:

T cell activation reduces the lethal dose of lipopolysaccharide 10-fold with major alterations in the immunological responses, while causing similar clinical outcomes.

Graphical Abstract

Correspondence: mtaylor15@northwell.edu, 350 Community Dr., Manhasset, NY 11030.

CONTRIBUTIONS

MDT performed all experiments, analyzed the data, wrote the manuscript and supervised all aspects of the study. TDF, OY, CEH, CAC, DEL, ANK, MNA, and MRB assisted in animal handling, in data analysis and in writing the manuscript. CSD assisted in experimental design, analysis of data and in writing.

DECLARATIONS OF INTERESTS

Disclosures: CSD is a consultant for Enlivex Therapeutics Inc, Jerusalem, Israel. This in no way influenced the content of the attached manuscript. The authors have no additional competing financial interests.

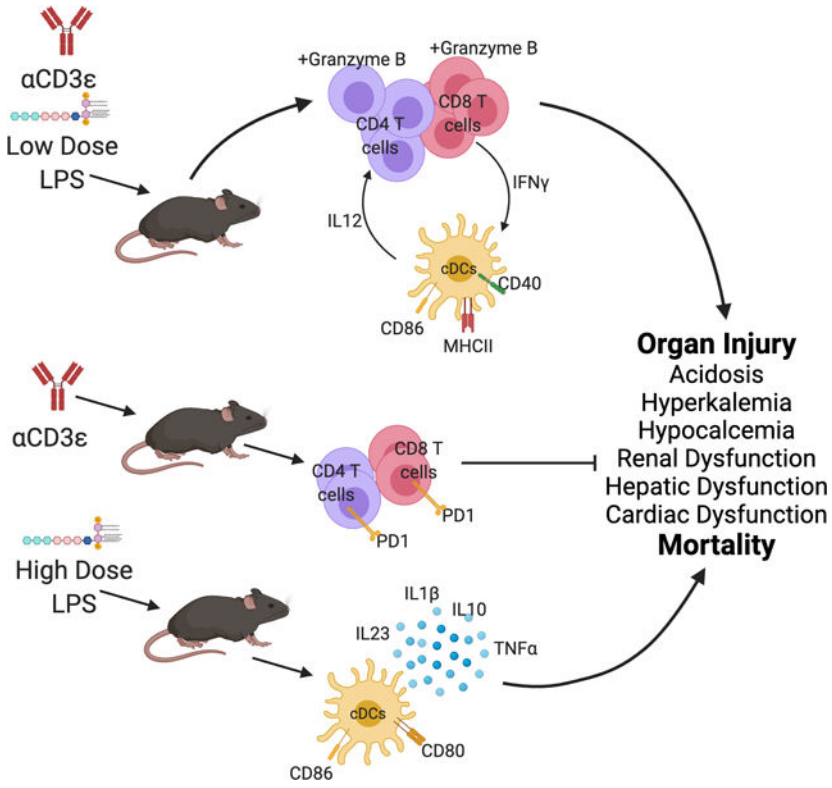

Keywords

T cells; Lipopolysaccharide; Organ Dysfunction; Interferon gamma; checkpoint inhibition; Dendritic cells

Introduction

Recent literature indicates that the adaptive immune system may play a more proximal role in modulating initial responses to pathogenic challenge than previously appreciated (1, 2). However, studying the contribution of the adaptive immune system to the initiation of the inflammatory response has been limited in part by lack of a well-developed memory T cell compartment in laboratory mice (3, 4). Our recent work in murine cecal ligation and puncture (CLP) demonstrated that induction of a robust memory T cell compartment prior to challenge influenced innate immune responses and increased organ dysfunction. Specifically, we noted that robust T cell receptor (TCR)-mediated activation of a high proportion of both the CD4 and CD8 T cell populations 35 days prior to procedure induced a memory T cell population that contributed to CLP-induced organ dysfunction (5).

Bacterial lipopolysaccharide (LPS)-mediated innate immune cell activation occurs, in part, via the toll-like receptor 4 (TLR4) pathway (6, 7). LPS is commonly administered to both animals and humans to induce inflammation (8–12). The murine response to LPS is characterized by rapid onset, low inter-animal variability and significant organ dysfunction, making it attractive for the study of responses to a severe insult (8, 13, 14). We therefore

used a combination of T cell activation and LPS to examine interactions between these two pathways and to dissect the mechanisms involved in T cell modulated organ dysfunction.

METHODS

Study Approval

All animal studies were approved by the Institutional Animal Care and Use Committee (IACUC #2017–039) and adhered to National Institutes of Health and Animal Research: Reporting of In Vivo Experiments (ARRIVE) guidelines.

Mice

C57Bl/6J male mice were obtained from the Jackson Laboratory (Bar Harbor, ME) and maintained in the animal facility at the Feinstein Institutes for Medical Research. Male mice were utilized to minimize weight variability and to avoid sex differences in LPS response (15–17). $CD4^{-/-}$ (B6.129S2-$CD4^{tm1Mak}$/J), $CD8^{-/-}$ (B6.129S2-$CD8a^{tm1Mak}$/J), $TCRab^{-/-}$ (B6.129S-$Tcra^{tm1Mom}$/J), and C3H/HeJ mice were obtained from the Jackson Laboratory and bred and maintained in our immunodeficient animal facility. Animals were housed together in our SPF facility for a minimum of 10 days prior to experimentation to ensure normalization of the microbiome (18).

Inflammatory Challenge

Ultra-LEAF isotype Armenian Hamster IgG control (Iso, Biolegend, San Diego, CA, Armenian Hamster clone HTK888; 50μg) and Ultra-LEAF Anti-mouse CD3ε Antibody (CD3, Biolegend, Armenian Hamster clone 145–2C11, 50μg) were administered to 14-week-old mice via retro-orbital venous sinus injection. Low dose LPS + isotype antibody treatment (LPSLo; from *Escherichia coli* O55:B5, Sigma-Aldrich L2880, 60μg), high dose LPS + isotype antibody treatment (LPSHi; 600μg), and CD3 + LPSLo treatment (CD3LPSLo) comprised the remaining groups. LPS was administered through intraperitoneal injection. Mice were followed for survival or sacrificed at 24 hrs. following challenge. Some treatments combined CD3 and CpG DNA (50μg, ODN 1826, InVivoGen, San Diego, CA) or CD3 and polyinosinic:polycytidylic acid (50μg, Sigma-Aldrich)(19).

In Vivo Cytokine Blockade

Mice were administered monoclonal antibody blockade at the time of inflammatory challenge and every three days following challenge. IFNγ (XMG1.2, 0.5mg), TNFα (XT3.11, 1mg) or IL12p40 (C17.8, 1mg) blocking antibodies were all obtained from BioXCell (Lebanon, NH), diluted from stock concentration in sterile PBS and administered through intraperitoneal injection. Full blocking doses as described in previous literature were used to identify cytokine effects (20, 21).

Leukocyte Isolation

Spleens were obtained from sacrificed mice and were immediately subjected to digestion with DNAse (100μg/mL) and Collagenase A (1mg/mL) in complete media for 30 minutes at 37°C. Cells were resuspended following filtration through a 70μm filter. Red blood

cells were lysed, white cells were counted using a Countess II Automated Cell Counter (ThermoFisher, Waltham, MA) and spleen cells were analyzed. A minimum of 2×10^6 events were analyzed for each sample.

In Vitro Activation Assay

Once splenic cells were homogenized, T cells were isolated by negative selection using the pan-T cell isolation kit (Miltenyi, Bergisch Gladbach, Germany). Total splenic cells and T cells were then stimulated with plate bound anti-CD3ε (5ug/ml) and LPS (500ng/ml) for 3 hours. Stimulation assay was performed alongside a control without stimulation to assess for background production as previously described (21). Cells were then stained for flow cytometric analysis.

Flow Cytometric Analysis

Once single-cell suspensions were obtained, cells were stained for flow cytometric analysis. Staining was performed with LIVE/DEAD fixable viability dye (Life Technologies) and the following antibodies: CD90.2, CD8a, CD4, CD69, Ki67, PD1, Ly6C, CD11c, Ly6G, MHCII, MHCI, CD86, CD80, CD40, IFNγ, IL12p40, and Granzyme B. Full antibody details are available in Supplemental Table 1. All flow cytometric analysis was performed on a BD LSR Fortessa 16-color cell analyzer and analyzed using FlowJo software version 10 (BD Bioscience, San Jose, CA). Gating strategies are listed in figure captions. Gating strategies are illustrated in Supp. Fig. 5A for CD4 T cells and CD8 T cells and Supp. Fig. 5B for innate immune cells.

Cytokine Production Assays

To assess cytokine production, once cells were in single cell suspension, cells were allowed to produce cytokine for 4 hours in the presence of Brefeldin A (2ug/ml) prior to staining, fixation and permeabilization. All stimulation assays were performed alongside a positive control and at the same time with samples from control mice to assess for background production as previously described (21).

ELISA Assays

Multiplex ELISA assays were performed by EVE Technologies (Calgary, AB, Canada). Findings were confirmed with BD OptEIA ELISA kits. Alanine Aminotransferase 1 ELISA Kit (Biovision, Milpitas, CA) and Bilirubin Assay Kit (Sigma-Aldrich, St Louis, MO) were used per manufacturer instructions.

In Vivo Imaging

Echocardiography was performed using the Vevo 3100 Ultrasound (Fujifulm Visual Sonics, Toronto, Canada). Echocardiography was analyzed by an experienced cardiologist according to a standard image collection protocol. Images were obtained under isoflurane anesthesia. Renal artery diameter and arterial velocity were also measured using ultrasonography. RBF was calculated with the following formula: $RBF = \pi(0.5 \times \text{renal artery diameter})^2 \times (\text{renal artery velocity})$.

Assessment of Electrolyte Abnormalities

All electrolytes and blood gas analysis were measured on whole blood immediately following collection using the iStat Chem8+ and CG4+ cartridges. This device is used for point-of-care measurement in clinical care (Abbott Point of Care Inc., Princeton, NJ).

Real-Time Polymerase Chain Reaction

Samples were stored in RNALater solution (Invitrogen) until total RNA was isolated (RNAeasy Mini Kit; Qiagen, Hilden, Germany). Quantitative real-time PCR was performed using an Applied Biosystems 7900HT Fast Real-Time PCR system. Primers were obtained from Applied Biosystems: TaqMan Gene Expression Assays Mm00441421_m1 (SCL10a1a), Mm01267415_m1 (SCLO1a1), and Mm99999915_g1 (GAPDH). Relative amplification to GAPDH was calculated using the ΔΔCT method, which measures the change in the relative quantification of a control mRNA gene in an experimental sample and a control sample to the change in the relative quantification of a target mRNA gene of interest in those same samples.

Statistical Analysis

Animal data were analyzed using one-way analysis of variance with Dunnett's post-hoc test for multiple comparisons where appropriate. Survival was calculated using the Spearman's Log Rank Test (Prism 7.0; GraphPad, San Diego, CA). For multiplex ELISA, statistical significance was tested by one-way ANOVA with Dunnett's post-hoc test for multiple comparisons compared to Iso treatment utilizing absolute numbers. All data shown are representative of at least two independent experiments to ensure results. The authors declare that all data supporting the findings of this study are available within the paper and its supplementary material.

Results

Combined TCR and TLR Activation increase Organ Injury and Mortality

Five treatment cohorts of C57Bl/6 mice were studied post-intervention: control isotype antibody treatment (Iso), anti-CD3ε T cell activating antibody treatment (CD3), low dose LPS (60μg) + isotype antibody treatment (LPSLo), high dose LPS (600μg) + isotype antibody treatment (LPSHi), and anti-CD3 + LPSLo treatment (CD3LPSLo). Use of these groups allowed us to assess the contributions of TLR4 (LPSLo, LPSHi) and TCR activation (CD3) individually or in combination (CD3LPSLo). The combination of CD3 and LPSHi was uniformly fatal at a very early timepoint.

Ten-day survival curves are depicted in Fig. 1A. As in previous reports, all mice in the Iso, CD3 and LPSLo cohorts survived (5, 22). Mortality at 48 hrs. was 55% in the LPSHi group and 70% in the CD3LPSLo group; CD3LPSLo had some continued attrition with a final mortality of 80%.

While it is known that LPS challenge disrupts organ function, the effects of T cell activation on the response to LPS has not been defined. Therefore, we examined general and organ-specific outcomes in our five cohorts. At 24 hrs. following intervention, systemic

abnormalities including hypothermia (Fig. 1B), metabolic acidosis (Fig. 1C), hyperkalemia (Fig. 1D), and hypocalcemia (Fig. 1E) were noted only in the CD3LPSLo group.

Hepatic dysfunction is most often quantified using serum transaminase and bilirubin levels. Alanine aminotransferase (ALT) was elevated in the LPSHi group. In contrast, bilirubin was elevated in the CD3LPSLo group (Fig. 1F). Hyperbilirubinemia may reflect impaired transport across hepatocytes, a process that is modulated by the sodium/bile acid cotransporter (NTCP, SCL10a1a) and the organic anion transporter protein 1 (OATP, SCLO1a1). We have previously demonstrated that decreased expression of the mRNA encoding these two proteins is a sensitive measure of hepatic dysfunction following CLP (23, 24). Expression of both transporters was lower in LPSHi and CD3LPSLo than in the other groups (Fig. 1G).

Serum creatinine and blood urea nitrogen (BUN) levels, used to indicate renal dysfunction, were significantly higher than Iso controls in the CD3LPSLo cohort (Fig. 1H). In addition, renal blood flow and renal artery diameter were greater in both the LPSHi and CD3LPSLo groups than in the other groups, with the most profound difference in the latter. (Fig. 1I). These differences are consistent with observations following CLP (25).

Finally, measures of cardiac function were similar in Iso, CD3, and LPSLo mice. However, stroke volume, fractional shortening and ejection fraction were lower in both LPSHi and CD3LPSLo mice than in the other groups. These abnormalities were more pronounced in CD3LPSLo animals (Fig. 1J).

In sum, while both the LPSHi and CD3LPSLo groups developed organ dysfunction, abnormalities were more pronounced in the CD3LPSLo cohort.

Interaction with TCR is TLR4-specific and involves both CD4 and CD8 T cells

To determine if other TLR agonists other than TLR4 interacted with TCR activation, additional cohorts were challenged with agonists for TLR9 (CpG DNA) and TLR3 (polyinosinic:polycytidylic acid, PolyI:C) at dosing consider equivalent to LPSLo in conjunction with anti-CD3ε administration (19). None of the animals subjected to these interventions died. Thus, only the combination of TCR and TLR4 activation was sufficient to cause fatalities (Supp. Fig. 1A). Administration of the combination of anti-CD3ε and low dose LPS to $CD4^{-/-}$ (B6.129S2-$CD4^{tm1Mak}$/J) and $CD8^{-/-}$ (B6.129S2-$CD8a^{tm1Mak}$/J) mice resulted in mortality equivalent to that seen in similarly-treated wild types (Supp. Fig. 1B). High dose LPS treatment caused equivalent mortality in $TCRab^{-/-}$ (B6.129S-$Tcra^{tm1Mom}$/J) mice as seen in wild types (Supp. Fig. 1C). No fatalities occurred following CD3LPSLo treatment of C3H/HeJ mice, which are resistant to LPS challenge due to a mutation in the TLR4 receptor (Supp. Fig. 1D).

TCR Activation Alters the Immunologic Response to Endotoxemia

While both LPSHi and CD3LPSLo groups developed significant pathology, the immunologic pathways activated by each challenge may differ. Therefore, we examined serum cytokine and chemokine levels in each group 24 hrs. following intervention (Fig. 2). All values from different treatment groups are presented as the fraction of the highest value.

A common set of cytokines (IL6, KC, RANTES, MCP1, MIP1α, MIP2, and M-CSF) were elevated in both the LPSHi and CD3LPSLo groups. Conversely, TNFα, IL23 (IL12p40), G-CSF, IL10 and IL1β, all more commonly associated with innate immune responses, were elevated in the LPSHi cohort only, while elevations in IFNγ, IL12p70, IL17, MIP1β, GM-CSF, IL3, and Leukemia inhibitory factor, possibly reflecting T cell activation, were confined to the CD3LPSLo cohort.

TCR Activation Increases the Classical Dendritic Cell Response to Endotoxemia

Because LPS stimulates innate immune activation through TLR signaling, we assessed splenic innate cell numbers 24 hrs. following challenge. Neutrophils were generally unaffected by LPS treatment; the number of neutrophils was only elevated in the CD3 group (Fig. 3A). Numbers of classical dendritic cells (cDCs, $CD11c^+/MHCII^+$) were lower in the CD3, LPSLo and LPSHi groups than in the Iso group but were similar to the Iso group in the CD3LPSLo group (Fig. 3B). The total numbers of splenic myeloid ($CD11b^+$) cells (Supp. Fig. 2A) and monocyte derived dendritic cells (MoDCs, $CD11b^+/MHCII^+$, Supp. Fig. 2B) were not significantly different in any of the five groups studied.

TLR agonists increase dendritic cell expression of antigen presentation molecules (e.g. MHC class I and class II) and costimulatory receptors (CD40, CD80, CD86). MHC class I expression on cDCs and MoDCs was higher than Iso in all groups (Fig. 3C). In contrast, MHC class II expression on cDCs and MoDCs was only significantly higher than Iso in the CD3LPSLo cohort (Fig. 3D). We also examined levels of the T cell costimulatory receptors CD86, CD80, and CD40. CD86 levels on cDCs were higher than Iso in both the LPSHi and CD3LPSLo cohorts (Fig. 3E). CD80 expression on cDCs and MoDCs was higher than Iso in the LPSLo, LPSHi and CD3LPSLo groups; expression in cDCs was highest the LPSHi cohort (Fig. 3F). In contrast, CD40 expression on cDCs and MoDCs was higher than Iso in the CD3, LPSLo, LPSHi and CD3LPSLo groups, and was highest in the CD3LPSLo cohort (Fig. 3G). In summary, co-ligand signaling in the LPSHi cohort was dominated by MHCI, CD86 and CD80, while MHCII, MHCI, CD86 and CD40 signaling predominated in the CD3LPSLo cohort. These findings indicate that T cell activation altered the innate response via alteration of antigen presentation and co-stimulation, which in turn fed back to alter T cell responses.

Previous reports have shown that cDCs are a major source of IL12p70 during immune responses. Activation of the IL12 receptor promotes transcription of IFNγ from T cells or other sources. This process then promotes further IL12p70 production by innate cells (26–28). Serum IL12p70 was elevated in the CD3LPSLo group (Fig. 2). To examine one possible source, we isolated splenic cells from each group and determined the number of $IL12p70^+$ cDCs present. Immediately *ex vivo,* without further stimulation, $IL12p70^+$ cDCs were rare in the Iso, CD3, LPSLo, and LPSHi cohorts. In contrast, the number of $IL12p70^+$ cDCs per spleen was higher in the CD3LPSLo cohort. This finding suggests that T cell activation, prompted by anti-CD3ε administration, contributed to IL12p70 production by activated cDCs (Fig. 3H).

T Cell Responses are Increased by Concurrent LPS Activation

In addition to elevation in IL12p70, high serum levels of IFNγ were noted in the CD3LPSLo cohort (Fig. 2). T cells are one potential source of IFNγ; production is driven by IL12p70 produced by activated cDCs (Fig. 3) (29, 30). Our data showed that IL12p70 expression was most profound in the CD3LPSLo cohort, suggesting that both the TCR and TLR4 pathways participated. To further characterize the effect of interactions between cDCs and T cells on IL12p70 and IFNγ production, we isolated both splenic T cells and total splenic cells (including T cells) from untreated mice. These cells were simultaneously stimulated with anti-CD3ε and LPS. Activation of T cells, as indicated by CD69 expression, was less pronounced on isolated T cells than in the T cells exposed to the entire splenic cell population (Fig. 4A, Supp. Fig. 3A). These findings indicate that T cell activation in response to CD3LPSLo is dependent on T cell interactions with another splenic cell type, presumably an APC.

In vivo assessment demonstrated that the numbers of splenic CD8 T cells in all treatment cohorts were lower than in the Iso cohort. The difference was most pronounced in the CD3 group (Fig. 4B). In contrast, the numbers of CD4 T cells were lower in the CD3 and LPSHi cohorts than in the Iso cohort; CD4 T cell numbers were not altered in the LPSLo or CD3LPSLo groups (Supp. Fig. 3B).

Overall, the number and percentage of activated (CD69 +) CD4 and CD8 splenic T cells was lower in the Iso group than in all other cohorts. The total number and the percentage of activated cells was highest in the CD3LPSLo cohort (Fig. 4C, Supp. Fig. 3C, 3D). Further, activation strength (CD69 MFI) of both CD8 and CD4 T cells was higher in the CD3LPSLo cohort than in all other groups, indicating that T cells in these groups received stronger induced activation signals (Fig. 4D, Supp. Fig. 3E). Thus, while there were fewer T cells in the CD3LPSLo cohort than in the Iso cohort, the total number of activated T cells, and the signal strength that induced activation, was higher in the CD3LPSLo group. (Fig. 4C, 4D and Supp. Fig. 3D, 3E).

T cell activation leads to proliferation, gain of effector functionality, and cytokine production. Expression of Ki67, a marker of active proliferation, was higher in the CD3 cohort than in the Iso cohort (Fig. 4E, Supp. Fig. 3F). In comparison, proliferation was lower than Iso in the LPSHi cohort. Ki67 expression in the CD3LPSLo group was higher than in the LPSHi group but was not different than in the Iso cohort (Fig. 4E, Supp. Fig. 3F). More activated (granzyme B^+) effector CD8 T cells were present in the CD3LPSLo group than in the Iso group (Fig. 4F, Supp. Fig. 3G). Granzyme B^+ CD4 T cells were noted in both the CD3 and the CD3LPSLo groups (Fig. 4F, Supp. Fig. 3G).

We noted previously that serum levels of IFNγ and IL12p70 were elevated in the CD3LPSLo groups (Fig. 2, 3). Both CD4 and CD8 T cells are known to produce IFNγ (26, 31). Therefore, we examined cytokine production by these cells in the five cohorts of mice. *Ex vivo* unstimulated production of IFNγ in the LPSLo, LPSHi and Iso cohorts was negligible. In contrast, IFNγ was produced by 3.5% of CD8 T cells and 3.4% of CD4 T cells in the CD3LPSLo group and in 7.2% of CD4 and 5.1% of CD8 T cells in the CD3 group. (Fig. 4G, Supp. Fig. 3H). However, the number of both CD4 and CD8 T cells in

the CD3LPSLo group was higher than in the CD3 group (Fig. 4B, Supp. Fig. 3B). Thus, a greater number of splenic T cells in the CD3LPSLo group produced IFNγ than in the CD3 group (Fig. 4G, Supp. Fig. 3H). Flow cytometric plots of granzyme B and IFNγ demonstrated that a statistically significant proportion of activated CD8 T cells gained both cytokine production and cytolytic functionality in response to CD3LPSLo (Fig. 4H). CD4 T cells demonstrated a similar gain in effector function (Supp. Fig. 3I).

LPS Prevents Checkpoint Inhibition of the T cell Response to Activation

Programmed cell death protein 1 (PD1) is expressed during T cell activation and, when engaged with its ligands PDL1 or PDL2, is a “checkpoint inhibitor” that protects against an inappropriate feed-forward activation cascade. PD1 is recognized as a marker of T cell exhaustion when T cells are exposed to chronic activation, but its expression on effector T cells is also a marker of acute activation. During acute priming to foreign antigen, PD1 limits overactivation. Further, PD1 limits aberrant activation of self-reactive T cells by raising the activation threshold. IFNγ is a negative regulator of PD1 (32). The expression of PD1 by T cells was examined in our five cohorts of mice. As noted, T cell activation in the CD3 group was less robust than that observed in CD3LPSLo cohort (Fig. 4D, Supp. Fig. 3E). TCR activation without LPS-mediated upregulation of activation signals (e.g., CD40, CD86, MHCI, MHCII) on APCs (Fig. 3) could fail to fully activate T cells. Therefore, we compared T cell PD1 and CD69 expression in the CD3 and CD3LPSLo cohorts. The percentage of cells expressing both PD1 and CD69 was higher than Iso in $CD8^+$ and $CD4^+$ T cells from the CD3 cohort but not from that observed in the CD3LPSLo cohort (Fig. 5A, Supp. Fig. 3K). The results were similar when the number of cells expressing both CD69 and PD1 was examined (Fig. 5B, Supp. Fig. 3K). In contrast, the number of $PD1^-CD69^+$ splenic CD4 and CD8 T cells in CD3LPSLo mice was significantly higher than what was observed in all other groups (Fig. 5C, Supp. Fig. 3K, flow cytometric plots shown in Fig. 5D and Supp. Fig. 3k). These data indicate that LPS modulates PD1 expression on T cells, likely effecting checkpoint inhibition during T cell activation in the CD3LPSLo cohort.

TNFα, IFNγ and IL12p40 contribute to Mortality in CD3LPSLo Mice and Organ Dysfunction can be alleviated by IFNγ blockade

We have shown that both IL12p70 and IFNγ production are elevated in CD3LPSLo (Fig. 2). To assess their contribution to mortality and organ function, we treated mice in the CD3LPSLo cohort with monoclonal blocking antibodies to IFNγ or to the IL12p40 subunit of IL12p70. Findings were compared to the effects of these antibodies on LPSHi mice. Because TNFα blockade in LPSHi is known to decrease mortality (as in Fig. 6A), anti-TNFα effects served as controls. Figure 6A demonstrates that, relative to untreated animals, TNFα blockade improved survival in both the LPSHi and CD3LPSLo groups. Mortality in LPSHi mice was not affected by IFNγ blockade, while survival was substantially higher in the treated CD3LPSLo group than in untreated controls. IL12p70 blockade in the LPSHi mice was almost uniformly fatal. Survival of CD3LPSLo mice was higher following IL12p70 blockade than in untreated animals; the difference was similar to that observed following IFNγ blockade. In CD3LPSLo mice, anti-IFNγ treatment reversed acidosis (Fig. 6B), serum potassium (Fig. 6C), and calcium levels (Fig. 6D), and values for indices of

hepatic, renal and cardiac function. Following IFNγ treatment these indices could not be distinguished from those observed in the Iso cohort (Fig. 6E-G).

T Cell Activation in CD3LPSLo Mice is Mediated by IFNγ, IL12p40 and TNFα

Improved survival and reduced organ dysfunction following treatment with antibodies blocking either IFNγ or IL12p70 suggest that these cytokines modulate observed changes in T cell responses. Therefore, we examined T cells following antibody administration in the CD3LPSLo group. The number of activated ($CD69^+$) CD4 and CD8 T cells was lower in CD3LPSLo mice treated with individual blockade of IFNγ, IL12p40 or TNFα (Fig. 7A, Supp. Fig. 4A) than in untreated mice. Similarly, the number of proliferating ($Ki67^+$) T cells was lower following blockade than in untreated animals (Fig. 7B, Supp. Fig. 4B). While the total number of activated $CD69^+$ T cells was lower in antibody-treated CD3LPSLo mice, the strength of activation in $CD69^+$ T cells was similar in untreated and treated animals (Supp. Fig. 4C). Thus, T cells were still being activated, but at a lower frequency. In addition, the number of splenic $IFN\gamma^+$ CD4 and CD8 T cells was lower following blockade of IFNγ, IL12p40 or TNFα (Fig. 7C, Supp. Fig. 4D). Blockade of IFNγ, IL12p40 or TNFα was also associated with a lower total number of activated ($CD69^+$) $PD1^-$ CD4 and CD8 T cells than in untreated mice (Fig.7D, Supp. Fig. 4E). Blockade of IFNγ, IL12p40 or TNFα did not affect the number of granzyme B^+ cytolytic CD8 T cells (Fig. 7E) but was associated with a significantly lower number of splenic cytolytic, (granzyme B^+) CD4 T cells than observed in untreated mice (Fig. 7F).

IFNγ, IL12p40 or TNFα Cytokine Blockade Attenuates Dendritic Cell MHCII and CD40 Upregulation

Cytotoxic CD4 T cells are generated by strong CD4 T cell/APC interactions (33). Therefore the lower number of cytotoxic CD4 T cells noted following blockade of IFNγ, IL12p40 or TNFα (Fig. 7F) might reflect an effect on CD4 T cell/APC interactions. Levels of the T cell co-ligand CD40 on splenic cDCs were lower following IFNγ, IL12p40 and TNFα blockade than in untreated mice (Fig. 7G). MHCII expression was also significantly lower on splenic cDCs from treated mice than in untreated animals (Fig. 7H).

Discussion

The studies detailed here demonstrate that T cell activation via the TCR pathway intensified the adverse effects of TLR4 immunopathology. Specifically, the combination of TCR and TLR4 pathway activation induced organ dysfunction and mortality equivalent to that seen following a 10-fold greater dose of LPS alone. Importantly, while adverse outcomes were similar in CD3LPSLo and LPSHi mice, the pathways involved differed. Thus, T cell responses modulate the response to severe inflammation.

LPS challenge is frequently used to model inflammation-induced organ dysfunction and mortality. While some direct effects of LPS on cellular pathways may lead to organ dysfunction, the contribution of other pathways, in particular those involving elements of the adaptive immune system, to cellular dysfunction has not been well-described. Laboratory mice lack a well-developed T cell memory compartment (3, 4). Therefore,

murine models of inflammatory disease may not appropriately reflect the role played by adaptive immunity (3, 4). Our recent work showed that induced adaptive immune memory altered the magnitude of organ dysfunction following cecal ligation and puncture (CLP) (1, 34). The experiments described here identify one potential mechanism. These studies indicate that the combination of TCR- and TLR4-mediated effects on T cell and dendritic cell interactions altered the response to LPS-induced inflammation and cellular dysfunction. Specifically, TCR-mediated activation of the IFNγ/IL12p70 axis amplified the effects of TLR4 activation on the innate immune response, which in turn, lowered the threshold for T cell responses through alteration of PD1-mediated checkpoint inhibition. Other investigators have noted that IFNγ from T cells and/or other sources drives an IL12p70-mediated feedforward activation loop (26–28). IL12p70 is known to promote cDC/T cell interactions through MHC class II and CD40, further driving T cell activation via stabilization of MHC/TCR complexes (29, 30). It is logical to postulate that similar processes are involved in the responses observed in the CD3LPSLo cohort.

The induction of cytotoxic CD4 T cells is particularly interesting. These cells recognize APCs (e.g., dendritic cells, monocytes and B cells) via interaction between MHC class II and CD4/TCR and efficiently eliminate APCs via perforin and granzyme B-mediated activation of the caspase-8 apoptosis pathway (35–39). Cytotoxic CD4 T cells have been associated with responses to severe inflammatory infections such as Dengue Fever and influenza (33, 36, 38, 39). Future studies will be required to investigate the contribution of these cells in eliminating activated APCs with elevated MHCII levels in our CD3LPSLo cohort (Fig. 3B). A cytotoxic CD4 T cell-mediated pruning of dendritic cells might contribute to sepsis-associated immunosuppression.

Our study does have limitations. We studied only the LPS/TLR4 pathway because it has been well-characterized and is a known component of inflammatory responses in humans. We did not see similar responses to TLR9 (ligand - CpG) or TLR3 (ligand - PolyI:C). Our findings are consistent with known effects of TLR4 ligands on dendritic cell maturation and IL12p70 expression (27). However, many other pathways may contribute to inflammatory responses. In addition, our use of an anti-CD3ε activating antibody creates an artificial (albeit highly efficient and well-controlled) T cell activation state that may not be reflective of the response to “real-world” challenges. The functional immune synapse formed between TCRs on T cells and the Fcγ receptor on APCs by the 145–2C11 anti-CD3ε antibody is likely stronger but briefer than most physiologic insults. Importantly, Fcγ ligation in isolation, present in the Iso cohort, did not elicit any of the effects observed with TCR activation by anti-CD3ε. Similarly, high-dose LPS is likely a more profound inflammatory insult than that observed in nature. Future studies should address the higher complexity that likely characterizes both murine and in human infections.

In summary, we have identified T cell activation as an important modifying factor in the innate immune response to LPS, an inflammatory stimulus. Our data demonstrate that cDC/T cell interactions can trigger an IFNγ/IL12p70 - mediated feedforward loop that overcomes the checkpoint inhibition and is associated with a CD4 cytolytic response. These processes contribute to morbidity and mortality in our model, suggesting the need for study in detrimental inflammation-associated responses in patients.

The findings in this and our previous studies indicate that T cell activation modulates innate immunity in ways that have not been accounted for when simplified, reductionist murine systems are used to model complex human disorders such as sepsis. A fuller understanding of complex immune networks may improve our understanding of clinical diseases. These insights may, in turn, allow us to more effectively apply animal models and translational studies to improve clinical outcomes.

Supplementary Material

Refer to Web version on PubMed Central for supplementary material.

ACKNOWLEDGEMENTS

MDT received funding from the NIH NIGMS K08GM132794 and from the Thrasher Research Fund Early Career Award 14734. CSD received funding from the NIH NIGMS R01GM121102.

References

1. Taylor MD, Fernandes TD, Kelly AP, Abraham MN, Deutschman CS. CD4 and CD8 T Cell Memory Interactions Alter Innate Immunity and Organ Injury in the CLP Sepsis Model. Front Immunol. 2020;11:563402.
2. Huggins MA, Sjaastad FV, Pierson M, Kucaba TA, Swanson W, Staley C, et al. Microbial Exposure Enhances Immunity to Pathogens Recognized by TLR2 but Increases Susceptibility to Cytokine Storm through TLR4 Sensitization. Cell Rep. 2019;28(7):1729–43 e5. [PubMed: 31412243]
3. Beura LK, Hamilton SE, Bi K, Schenkel JM, Odumade OA, Casey KA, et al. Normalizing the environment recapitulates adult human immune traits in laboratory mice. Nature. 2016;532(7600):512–6. [PubMed: 27096360]
4. Abolins S, King EC, Lazarou L, Weldon L, Hughes L, Drescher P, et al. The comparative immunology of wild and laboratory mice, Mus musculus domesticus. Nat Commun. 2017;8:14811. [PubMed: 28466840]
5. Taylor MD, Brewer MR, Deutschman CS. Induction of diverse T cell memory through antibody-mediated activation in mice. Eur J Immunol. 2020;50(11):1838–40. [PubMed: 32627182]
6. Chow JC, Young DW, Golenbock DT, Christ WJ, Gusovsky F. Toll-like receptor-4 mediates lipopolysaccharide-induced signal transduction. J Biol Chem. 1999;274(16):10689–92. [PubMed: 10196138]
7. Poltorak A, He X, Smirnova I, Liu MY, Van Huffel C, Du X, et al. Defective LPS signaling in C3H/HeJ and C57BL/10ScCr mice: mutations in Tlr4 gene. Science. 1998;282(5396):2085–8. [PubMed: 9851930]
8. Lilley E, Armstrong R, Clark N, Gray P, Hawkins P, Mason K, et al. Refinement of animal models of sepsis and septic shock. Shock. 2015;43(4):304–16. [PubMed: 25565638]
9. Fink MP, Heard SO. Laboratory models of sepsis and septic shock. Journal of Surgical Research. 1990;49(2):186–96. [PubMed: 2199735]
10. Zanin-Zhorov A, Tal-Lapidot G, Cahalon L, Cohen-Sfady M, Pevsner-Fischer M, Lider O, et al. Cutting edge: T cells respond to lipopolysaccharide innately via TLR4 signaling. J Immunol. 2007;179(1):41–4. [PubMed: 17579019]
11. Tawfik DM, Lankelma JM, Vachot L, Cerrato E, Pachot A, Wiersinga WJ, et al. Comparison of host immune responses to LPS in human using an immune profiling panel, in vivo endotoxemia versus ex vivo stimulation. Sci Rep. 2020;10(1):9918. [PubMed: 32555232]
12. Zielen S, Trischler J, Schubert R. Lipopolysaccharide challenge: immunological effects and safety in humans. Expert Rev Clin Immunol. 2015;11(3):409–18. [PubMed: 25655761]
13. Stortz JA, Raymond SL, Mira JC, Moldawer LL, Mohr AM, Efron PA. Murine Models of Sepsis and Trauma: Can We Bridge the Gap? ILAR J 2017;58(1):90–105. [PubMed: 28444204]

14. von Asmuth EJ, Maessen JG, van der Linden CJ, Buurman WA. Tumour necrosis factor alpha (TNF-alpha) and interleukin 6 in a zymosan-induced shock model. Scand J Immunol. 1990;32(4):313–9. [PubMed: 2237286]
15. Card JW, Carey MA, Bradbury JA, DeGraff LM, Morgan DL, Moorman MP, et al. Gender differences in murine airway responsiveness and lipopolysaccharide-induced inflammation. J Immunol. 2006;177(1):621–30. [PubMed: 16785560]
16. Kuo SM. Gender Difference in Bacteria Endotoxin-Induced Inflammatory and Anorexic Responses. PLoS One. 2016;11(9):e0162971.
17. Moeinpour F, Choudhry MA, Kawasaki T, Timares L, Schwacha MG, Bland KI, et al. 17 Beta-estradiol normalizes Toll receptor 4, mitogen activated protein kinases and inflammatory response in epidermal keratinocytes following trauma-hemorrhage. Mol Immunol. 2007;44(13):3317–23. [PubMed: 17403539]
18. Fay KT, Klingensmith NJ, Chen CW, Zhang W, Sun Y, Morrow KN, et al. The gut microbiome alters immunophenotype and survival from sepsis. FASEB J. 2019;33(10):11258–69. [PubMed: 31306584]
19. Behrens EM, Canna SW, Slade K, Rao S, Kreiger PA, Paessler M, et al. Repeated TLR9 stimulation results in macrophage activation syndrome-like disease in mice. J Clin Invest. 2011;121(6):2264–77. [PubMed: 21576823]
20. Jordan MB, Hildeman D, Kappler J, Marrack P. An animal model of hemophagocytic lymphohistiocytosis (HLH): CD8+ T cells and interferon gamma are essential for the disorder. Blood. 2004;104(3):735–43. [PubMed: 15069016]
21. Taylor MD, Burn TN, Wherry EJ, Behrens EM. CD8 T Cell Memory Increases Immunopathology in the Perforin-Deficient Model of Hemophagocytic Lymphohistiocytosis Secondary to TNF-alpha. Immunohorizons. 2018;2(2):67–73. [PubMed: 29795796]
22. Tateda K, Matsumoto T, Miyazaki S, Yamaguchi K. Lipopolysaccharide-induced lethality and cytokine production in aged mice. Infect Immun. 1996;64(3):769–74. [PubMed: 8641780]
23. Abraham MN, Kelly AP, Brandwein AB, Fernandes TD, Leisman DE, Taylor MD, et al. Use of Organ Dysfunction as a Primary Outcome Variable Following Cecal Ligation and Puncture: Recommendations for Future Studies. Shock. 2020;54(2):168–82. [PubMed: 31764625]
24. Andrejko KM, Raj NR, Kim PK, Cereda M, Deutschman CS. IL-6 modulates sepsis-induced decreases in transcription of hepatic organic anion and bile acid transporters. Shock. 2008;29(4):490–6. [PubMed: 17724432]
25. Leisman DE, Fernandes TD, Bijol V, Abraham MN, Lehman JR, Taylor MD, et al. Impaired angiotensin II type 1 receptor signaling contributes to sepsis induced acute kidney injury. Kidney Int. 2020.
26. Ma XJ, Chow JM, Gri G, Carra G, Gerosa F, Wolf SE, et al. The interleukin 12 p40 gene promoter is primed by interferon gamma in monocytic cells. Journal of Experimental Medicine. 1996;183(1):147–57. [PubMed: 8551218]
27. Roses RE, Xu S, Xu M, Koldovsky U, Koski G, Czerniecki BJ. Differential Production of IL-23 and IL-12 by Myeloid-Derived Dendritic Cells in Response to TLR Agonists. The Journal of Immunology. 2008;181(7):5120–7. [PubMed: 18802116]
28. Soudja SM, Chandrabos C, Yakob E, Veenstra M, Palliser D, Lauvau G. Memory-T-cell-derived interferon-gamma instructs potent innate cell activation for protective immunity. Immunity. 2014;40(6):974–88. [PubMed: 24931122]
29. Benjamim CF, Hogaboam CM, Lukacs NW, Kunkel SL. Septic Mice Are Susceptible to Pulmonary Aspergillosis. The American Journal of Pathology. 2003;163(6):2605–17. [PubMed: 14633632]
30. Roquilly A, Broquet A, Jacqueline C, Gautreau L, Segain JP, de Coppet P, et al. Toll-like receptor-4 agonist in post-haemorrhage pneumonia: role of dendritic and natural killer cells. Eur Respir J. 2013;42(5):1365–78. [PubMed: 23314895]
31. Rottinghaus EK, Vesosky B, Turner J. Interleukin-12 is sufficient to promote antigen-independent interferon-gamma production by CD8 T cells in old mice. Immunology. 2009;128(1 Suppl):e679–90.

32. Sharpe AH, Pauken KE. The diverse functions of the PD1 inhibitory pathway. Nat Rev Immunol. 2018;18(3):153–67. [PubMed: 28990585]

33. Jellison ER, Kim SK, Welsh RM. Cutting edge: MHC class II-restricted killing in vivo during viral infection. J Immunol. 2005;174(2):614–8. [PubMed: 15634878]

34. Taylor MD, Brewer MR, Nedeljkovic-Kurepa A, Yang Y, Reddy KS, Abraham MN, et al. CD4 T Follicular Helper Cells Prevent Depletion of Follicular B Cells in Response to Cecal Ligation and Puncture. Front Immunol. 2020;11:1946. [PubMed: 32903485]

35. Appay V, Zaunders JJ, Papagno L, Sutton J, Jaramillo A, Waters A, et al. Characterization of CD4(+) CTLs ex vivo. J Immunol. 2002;168(11):5954–8. [PubMed: 12023402]

36. Brown DM, Lee S, Garcia-Hernandez Mde L, Swain SL. Multifunctional CD4 cells expressing gamma interferon and perforin mediate protection against lethal influenza virus infection. J Virol. 2012;86(12):6792–803. [PubMed: 22491469]

37. Juno JA, van Bockel D, Kent SJ, Kelleher AD, Zaunders JJ, Munier CM. Cytotoxic CD4 T Cells-Friend or Foe during Viral Infection? Front Immunol. 2017;8:19. [PubMed: 28167943]

38. Tian Y, Babor M, Lane J, Schulten V, Patil VS, Seumois G, et al. Unique phenotypes and clonal expansions of human CD4 effector memory T cells re-expressing CD45RA. Nat Commun. 2017;8(1):1473. [PubMed: 29133794]

39. Weiskopf D, Bangs DJ, Sidney J, Kolla RV, De Silva AD, de Silva AM, et al. Dengue virus infection elicits highly polarized CX3CR1+ cytotoxic CD4+ T cells associated with protective immunity. Proc Natl Acad Sci U S A. 2015;112(31):E4256–63. [PubMed: 26195744]

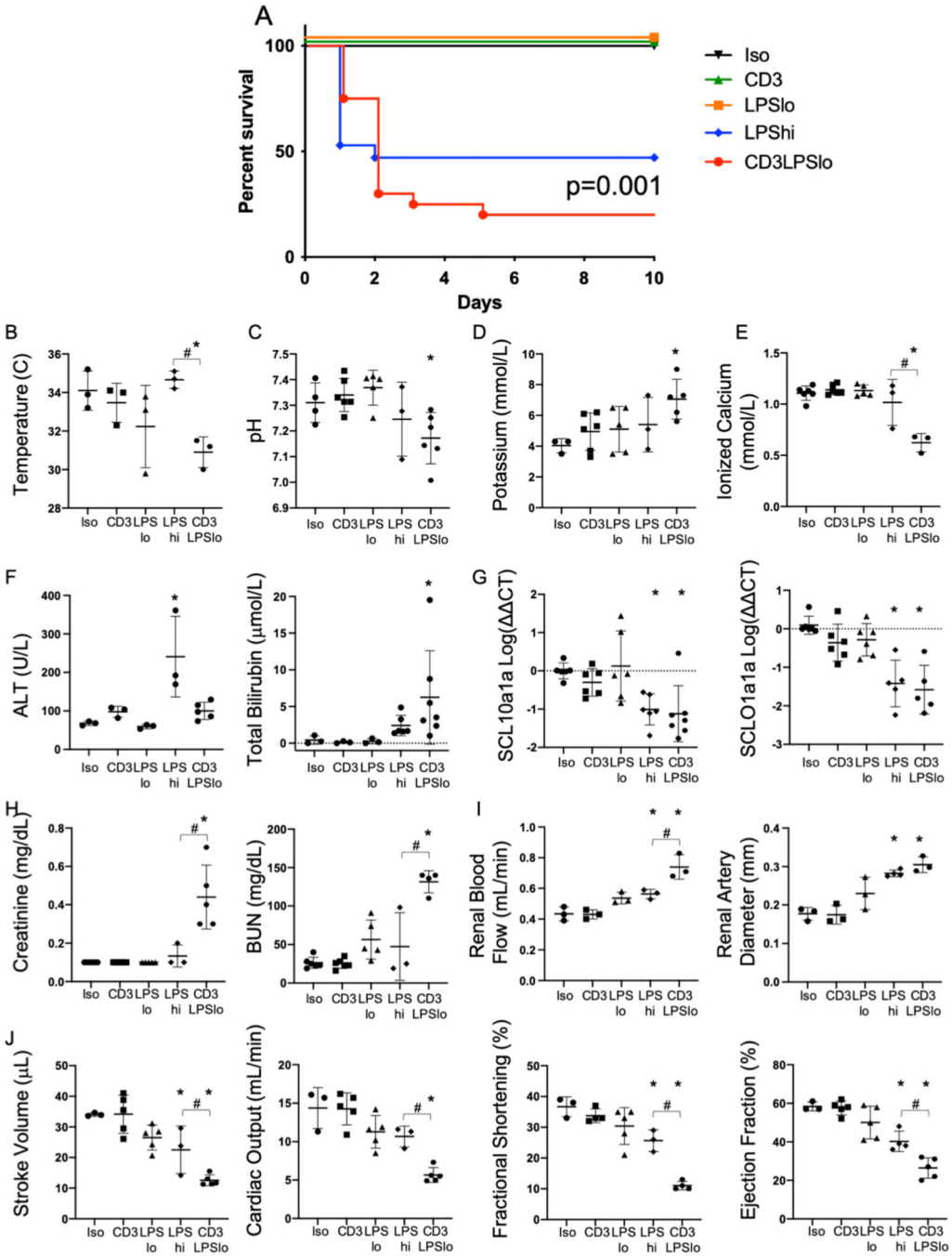

Figure 1. Effects of T cell Receptor Activation on LPS-induced Survival and Organ Injury.

Five treatment groups of C57Bl/6 mice were studied: Iso - control isotype antibody treatment (50μg), CD3 - anti-CD3ε T cell activating antibody treatment (clone 145–2C11, 50μg), LPSLo - low dose LPS (60μg) + isotype antibody treatment, LPSHi - high dose LPS (600μg) + isotype antibody treatment, CD3LPSLo - CD3 + LPSLo treatment. Animals were either observed until demise (or for up to ten days) or were studied at 24 hrs. following treatment. Data as mean ± standard deviation. * = $p<0.05$ compared to Iso # = $p<0.05$ LPSHi vs. CD3LPSLo. Spearman's Log-rank test for Fig1A; all other data examined using

one-way ANOVA with Dunnett correction for multiple comparisons. Figures representative of at least two independent experiments.

A. Ten-day Survival following challenge. N=5–11/group.

B. Rectal temperature (°C). N=3/group.

C. Serum pH. N=4–6/group.

D. Serum potassium level (mmol/L) N=4–6/group.

E. Serum ionized calcium level (mmol/L). N=4–6/group.

F. Serum levels of alanine aminotransferase (U/L) and total bilirubin (μmol/L). N=3–7/group.

G. Relative hepatic abundance of mRNA encoding Sodium/Bile Acid Cotransporter (SCL10a1a, Left) and Organic Anion Transporter (SCLO1a1, Right). ΔΔCT values of each sample normalized to GAPDH to account for loading, mean value for abundance of control specimen arbitrarily set at unity. Shown as Log10. N=3–4/group.

H. Left: Serum Creatinine (mg/dL). Right: Blood urea nitrogen (BUN, mg/dL). N=4–6/group.

I. Left: Renal blood flow (mL/min). Right: Renal artery diameter (mm). N=4–6/group.

J. Echocardiographic Parameters. Left – Stroke Volume (μL), Left Middle - Cardiac Output (mL/min), Right Middle - Fractional Shortening (%), Right – Ejection Fraction (%)). N=3/group.

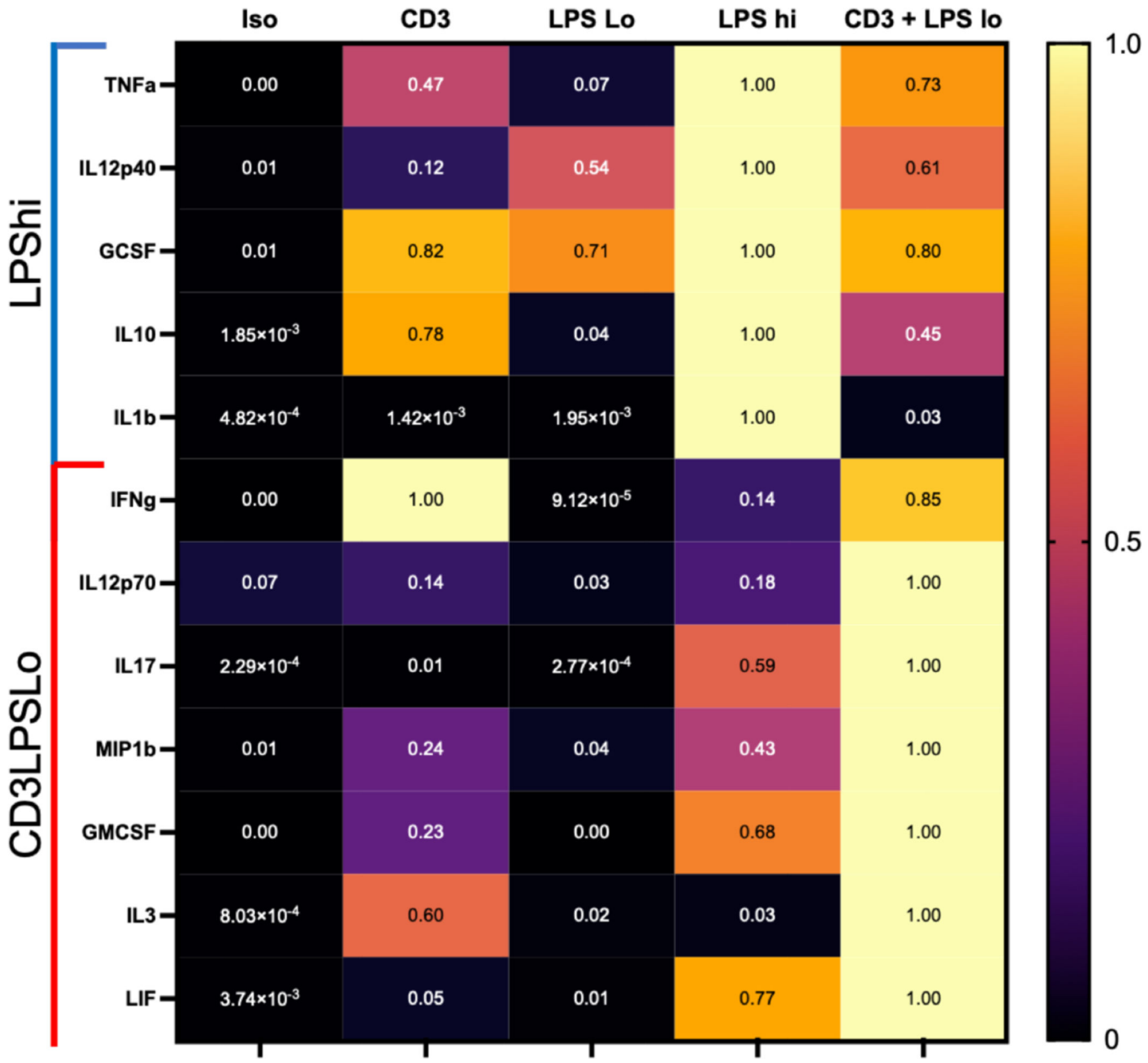

Figure 2. Effects of T cell Receptor Activation on the Serum Cytokine Response to LPS.

Abbreviations for the five treatment groups of C57Bl/6 mice as detailed in Fig. 1. Data obtained 24 hrs. following treatment. Serum cytokines determined using multiplex ELISA, confirmed using individual ELISAs. Data shown as percent cytokine levels above or below serum levels in Iso cohort. Significance ($p<0.05$) relative to Iso determined using one-way ANOVA with Dunnett correction for multiple comparisons on absolute values. LPSHi - cytokines that were significantly different than Iso cohort in response to 600μg of LPS. CD3LPSLo - cytokines that were significantly different than Iso cohort in response to anti-CD3ε T cell activating antibody (50μg) + 60μg LPS.

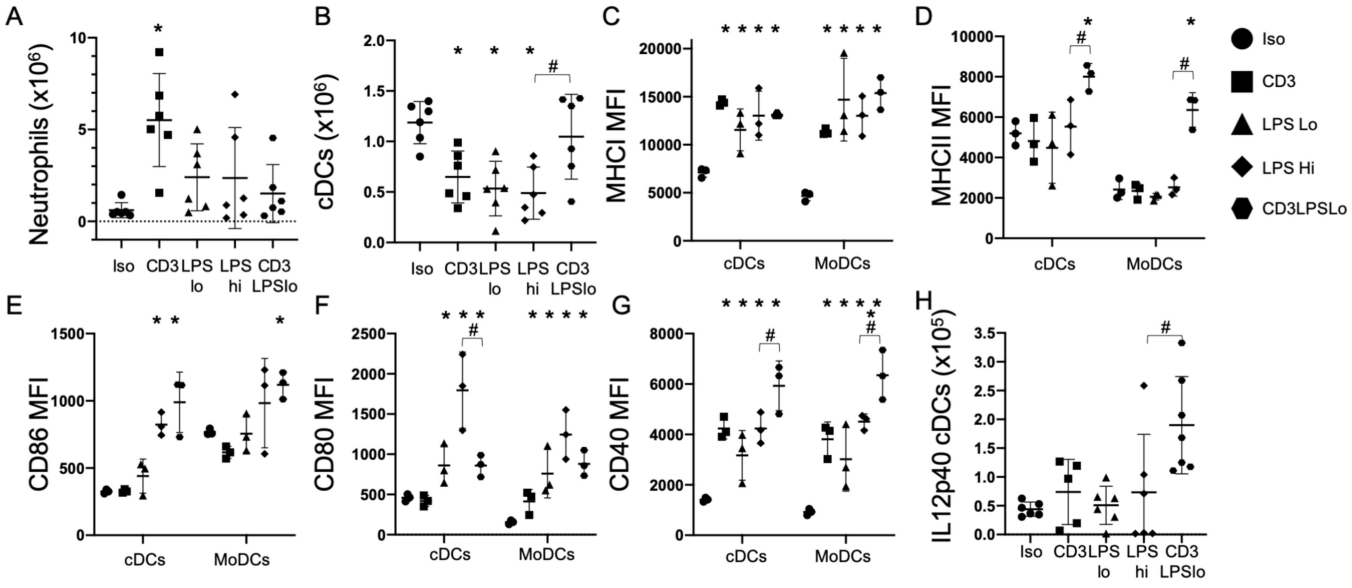

Figure 3. Effects of T cell Receptor Activation on the Splenic Innate Immune Response to LPS.

Abbreviations for the five treatment groups of C57Bl/6 mice as detailed in Fig. 1.

Data obtained 24 hrs. post treatment. Gating: Neutrophils: FSC/SSC, singlets, Live, $CD11b^{+}/Ly6G^{+}$; also Ly6Cint; Classical Dendritic Cells: FSC/SSC, singlets, Live, $CD11c^{+}/CD11b^{+/-}$, $CD11c^{+}/MHCII^{+}$, MHCI, MHCII, CD86, CD80, CD40, IL12p40. Monocyte-derived Dendritic Cells (MoDCs): FSC/SSC, singlets, Live, $CD11c^{-}/CD11b^{+}$, $CD11b^{+}/Ly6G^{-}$, $CD11b^{+}/MHCII^{+}$, MHCI, MHCII, CD86, CD80, CD40. Full gating strategy shown in Supp. Fig. 5B. Data as mean ± standard deviation. Significance determined using one-way ANOVA with Dunnett correction for multiple comparisons. * = $p<0.05$ relative to Iso, # = $p<0.05$ LPSHi vs. CD3LPSLo. Figures representative of at least two independent experiments.

A. Number of neutrophils obtained from the spleen. N=6/group.

B. Number of classical dendritic cells obtained from the spleen. N=6/group.

C. MHCI MFI for cDCs and MoDCs. N=3/group.

D. MHCII MFI for cDCs and MoDCs. N=3/group.

E. CD86 MFI for cDCs and MoDCs. N=3/group.

F. CD80 MFI for cDCs and MoDCs. N=3/group.

G. CD40 MFI for cDCs and MoDCs. N=3/group.

H. Number of splenic classical dendritic cells producing IL12p40 *ex vivo* without stimulation. N=6/group.

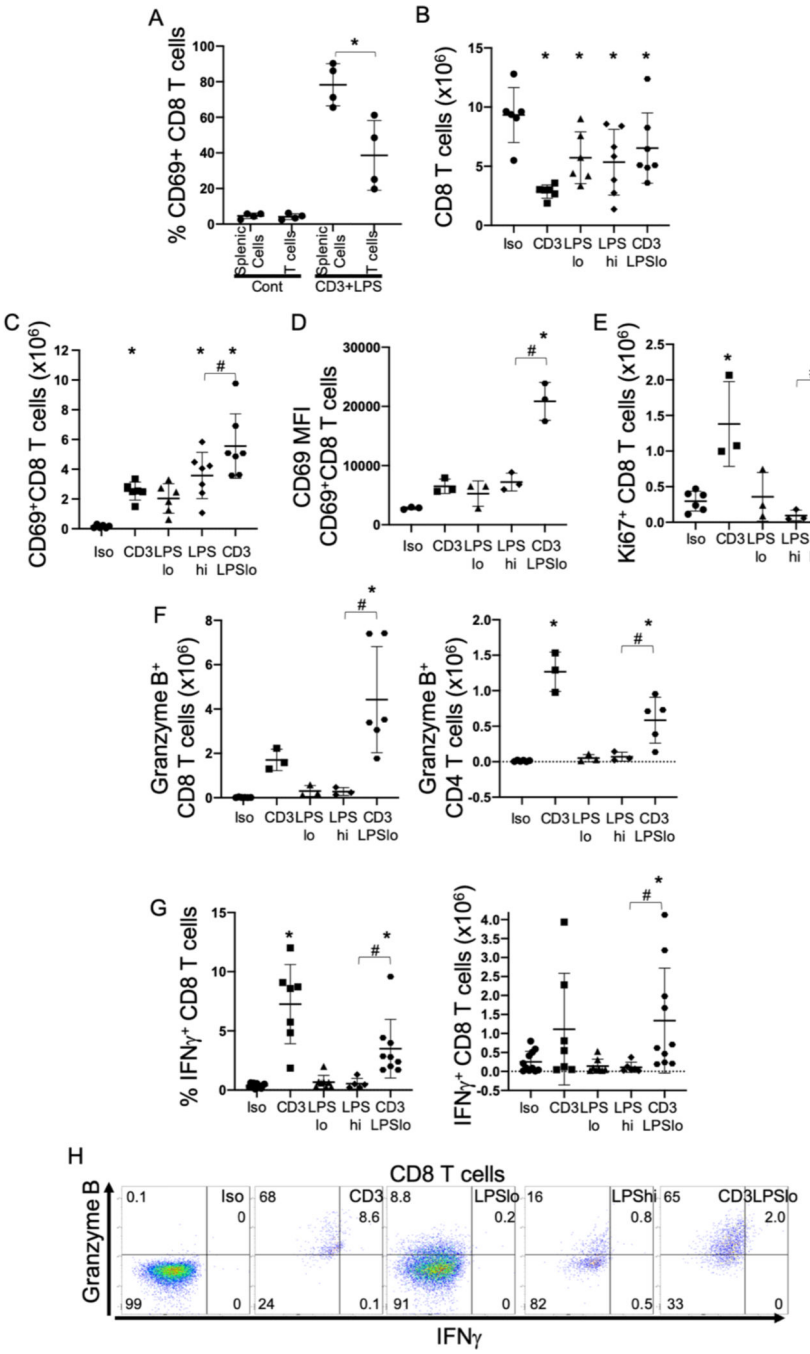

Figure 4. Effects of T cell Receptor Activation on the Splenic T cell Immune Response to LPS.

Splenic cells were obtained from C57Bl/6 mice and T cells were isolated by negative selection column separation. Cells were stimulated *in vitro* with specific stimuli and analyzed by flow cytometry. Abbreviations for the five treatment groups of C57Bl/6 mice as detailed in Fig. 1. Animals were studied at 24 hrs. following treatment. Gating: FSC/SSC, singlets, Live, CD90/CD4, CD90/CD8, CD69, Ki67, Granzyme B, IFNγ. Full gating strategy shown in Supp. Fig. 5A. Data as mean ± standard deviation. Significance determined using one-way ANOVA with Dunnett correction for multiple comparisons. * =

p<0.05 relative to Iso # = p<0.05 LPSHi vs. CD3LPSLo. Figures representative of at least two independent experiments.

A. Percent $CD69^+$ of CD8 T cells following *in vitro* stimulation of total splenic cells or isolated T cells. N=4/group.

B. Number of CD8 T cells obtained from the spleen. N=6/group.

C. Number of $CD69^+$ CD8 T cells obtained from the spleen. N=6/group.

D. CD69 MFI for splenic $CD69^+$ CD8 T cells. N=3/group.

E. Number of $Ki67^+$ CD8 T cells obtained from the spleen. N=6/group.

F. Number of Granzyme B^+ CD8 (Right) and CD4 (Left) T cells obtained from the spleen. N=6/group.

G. Percent (Left) and total (Right) CD8 T cells spontaneously producing IFNγ *ex vivo* without stimulation. Cells treated with Brefeldin A for four hours prior to intracellular cytokine staining. N=6–10/group.

H. Flow cytometric plots following treatment showing IFNγ/Granzyme B in CD8 T cells. Numbers represent average percentage of 3–4 replicates.

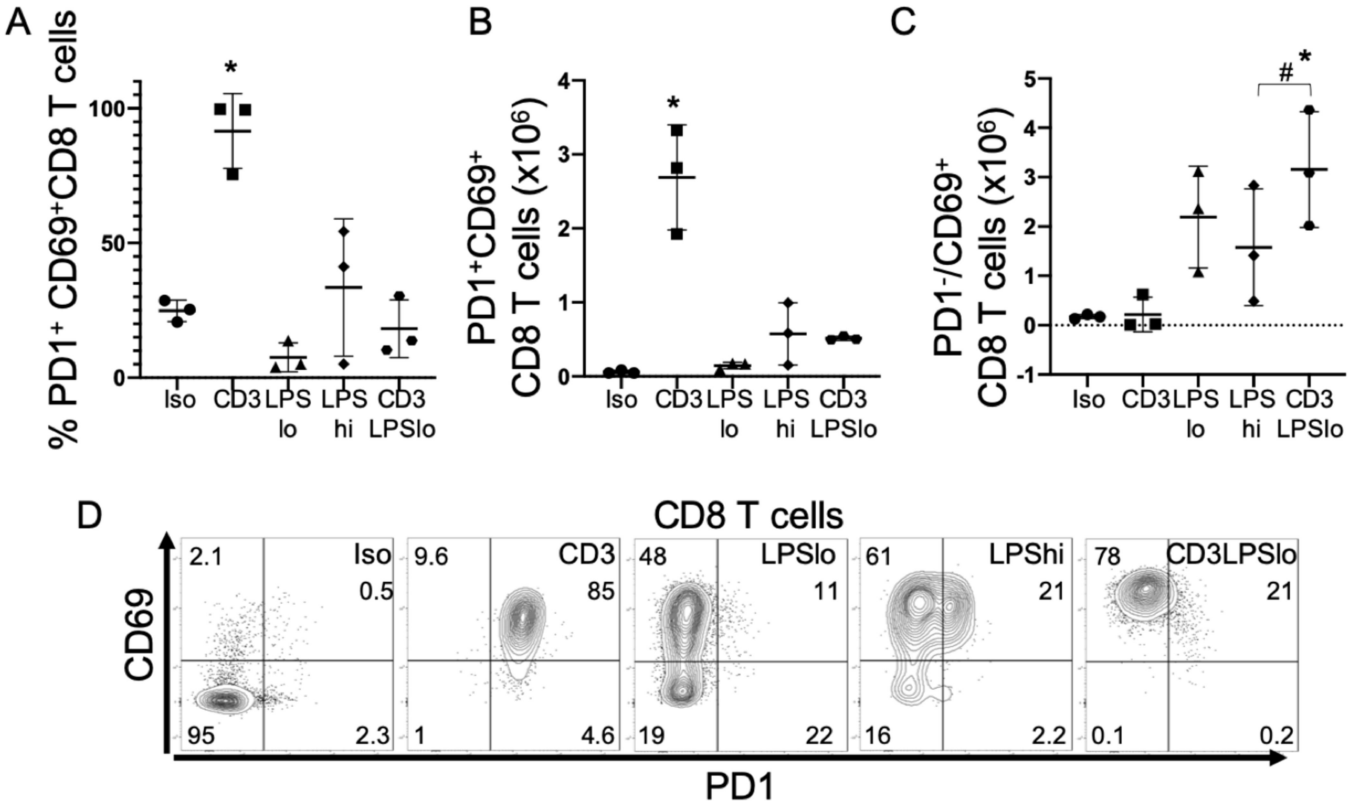

Figure 5. Effects of LPS on Splenic T cell Checkpoint Induction in Response to T cell Receptor Activation.

Abbreviations for the five treatment groups of C57Bl/6 mice as detailed in Fig. 1. Animals were studied at 24 hrs. following treatment. Gating: FSC/SSC, singlets, Live, CD90/CD4, CD90/CD8, CD69/PD1. Full gating strategy shown in Supp. Fig. 5(A). Data as mean ± standard deviation.

* = Significance determined using one-way ANOVA with Dunnett correction for multiple comparisons. $p<0.05$ relative to Iso # = $p<0.05$ LPSHi vs. CD3LPSLo. Figures representative of at least two independent experiments.

A. Percent of splenic $CD69^+$ CD8 T cells expressing PD1. N=3/group.

B. Number of $PD1^+CD69^+$ CD8 T cells obtained from the spleen. N=3/group.

C. Number of $PD1^-CD69^+$ CD8 T cells obtained from the spleen. N=3/group

D. Flow cytometric plots following treatment showing CD69/PD1 in CD8 T cells. Numbers represent average percentage of 3–4 replicates.

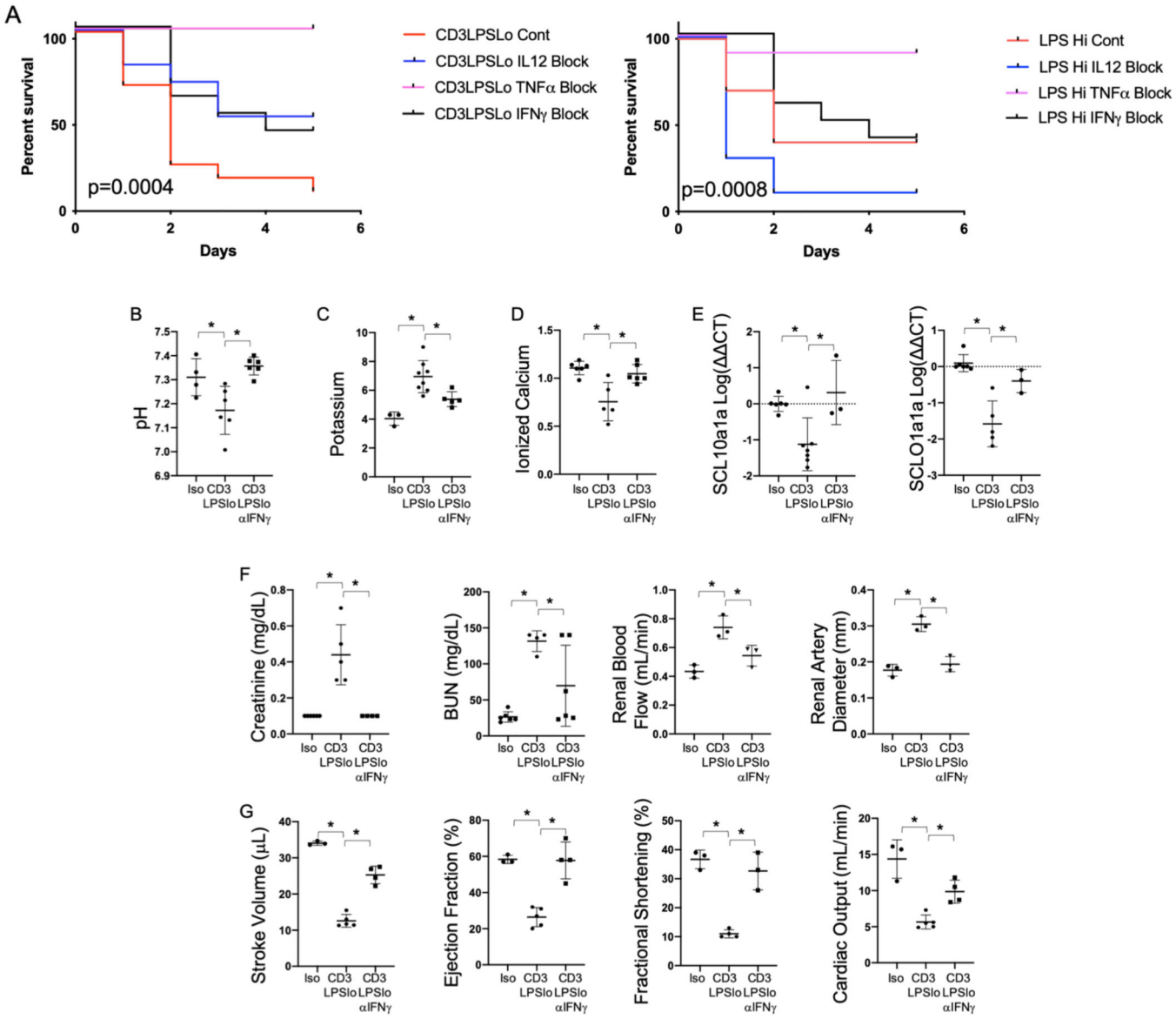

Figure 6. Effects of Cytokine Blockade on TCR modulated LPS-Induced Organ Injury.

Iso, CD3LPSLo, or LPSHi mice treated with blocking antibodies to IFNγ (XMG1.2, 0.5mg), TNFα (XT3.11, 1mg) or IL12p40 (C17.8, 1mg) on day 1 of challenge and every 3 days following. Mice studied for 10-day survival or 24 hrs. following treatment. Data as mean ± standard deviation. Statistically significant differences in survival determined using Spearman's Log-rank test. Significance for other studies determined using one-way ANOVA with Dunnett correction for multiple comparisons. * = $p<0.05$ relative to CD3LPSLo. . Figures representative of at least two independent experiments.

A. Ten-day Survival following challenge with CD3LPSLo (Left) or LPSHi (Right). N=5–11/group.

B. Serum pH (N=4–6/group).

C. Serum potassium level (mmol/L). N=4–6/group.

D. Serum ionized calcium level (mmol/L). N=4–6/group.

E. Relative hepatic abundance of mRNA encoding Sodium/Bile Acid Cotransporter (SCL10a1a, Left) and Organic Anion Transporter (SCLO1a1, Right). ΔΔCT values of each sample normalized to GAPDH to account for loading, mean value for abundance of control specimen arbitrarily set at unity. Shown as Log10. N= 3–4/group.
F. Left - Serum Creatinine (mg/dL), Left Middle - blood urea nitrogen (BUN, mg/dL), Right Middle - renal blood flow (mL/min), Right - renal artery diameter (mm). N=4–6/group.
G. Cardiac Function Parameters as assessed by echocardiography under isoflurane anesthesia. Left – Stroke Volume (μL), Left Middle - Cardiac Output – mL/min, Right Middle - Fractional Shortening (%), Right – Ejection Fraction (%). N=3/group.

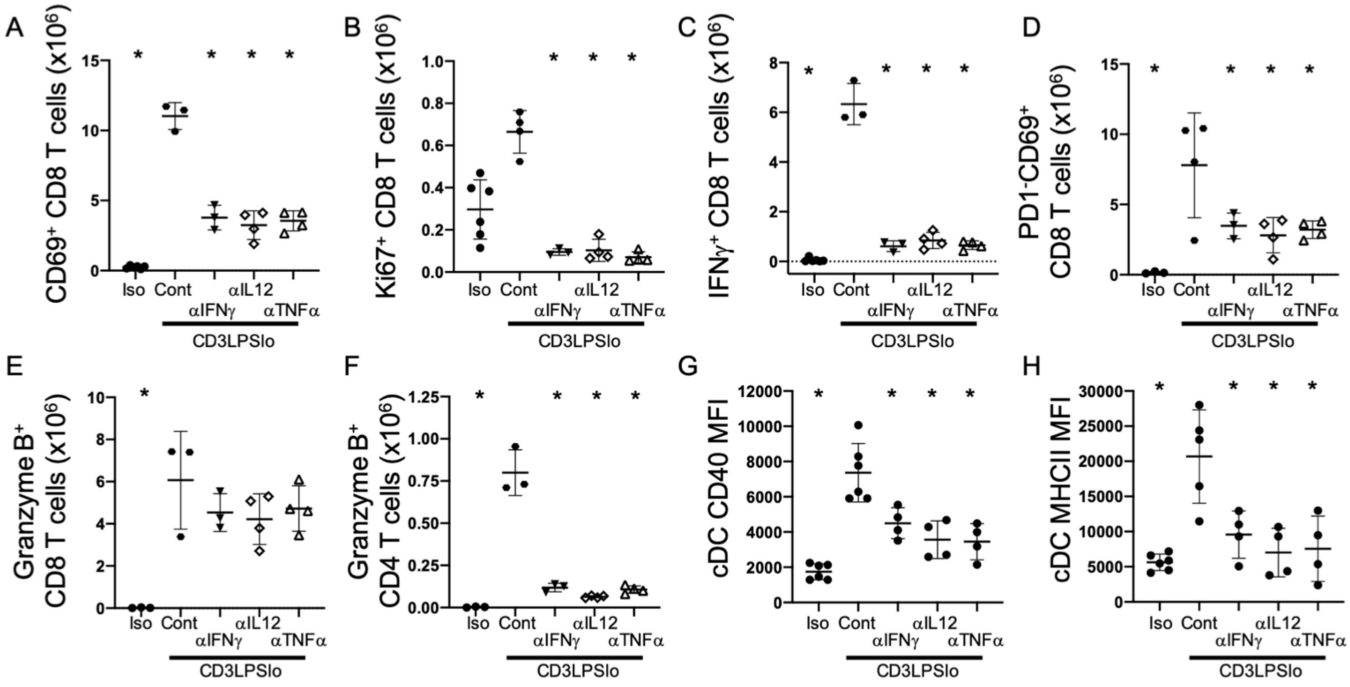

Figure 7. Effects of Cytokine Blockade on the T cell and Innate Immune Response to TCR modulated LPS Challenge.

Iso, CD3LPSLo, or LPSHi mice treated with blocking antibodies to IFNγ, TNFα or IL12p40 as per previous figure on day 1 of challenge and every 3 days following. Mice studied 24 hrs. following treatment. Gating: T cells: FSC/SSC, singlets, Live, CD90/CD4, CD90/CD8, CD69, Ki67, Granzyme B, PD1. Classical Dendritic Cells: FSC/SSC, singlets, Live, $CD11c^{+}/CD11b^{+/-}$, $CD11c^{+}/MHCII^{+}$, MHCII, CD40. Data as mean ± standard deviation, full gating strategy shown in Supp. Fig. 5B and 6. Significance determined using one-way ANOVA with Dunnett correction for multiple comparisons; * = $p<0.05$ relative to CD3LPSLo. Figures representative of at least two independent experiments.

A. Number of $CD69^{+}$ CD8 T cells obtained from the spleen. N=3–4/group.

B. Number of $Ki67^{+}$ CD8 T cells obtained from the spleen. N=3–4/group.

C. Total splenic CD8 T cells producing IFNγ *ex vivo* without stimulation. Cells treated with Brefeldin A for four hours prior to intracellular cytokine staining. N=3–4/group.

D. Number of $PD1^{-}CD69^{+}$ CD8 T cells obtained from the spleen. N=3–4/group.

E. Number of Granzyme B^{+} CD8 T cells obtained from the spleen. N=3–4/group.

F. Number of Granzyme B^{+} CD4 T cells obtained from the spleen. N=3–4/group.

G. CD40 MFI for cDCs. N=6/group.

H. MHCII MFI for cDCs and MoDCs. N=6/group.